PREPRINT version

Future heat extremes likely to have been underestimated

N. Freychet[1], G. Hegerl[1], D. Mitchell[2], M. Collins[3]

[1]School of Geosciences, University of Edinburgh, Edinburgh, UK

[2]School of Geographical Sciences, University of Bristol, Bristol, UK

[3]College of Engineering, Mathematics and Physical Sciences, *University of Exeter, Exeter, UK*

Corresponding author: nicolas.freychet@ed.ac.uk

In a warming world, temperature extremes are expected to show a distinguishable change over much of the globe[1] and in many regions this change has already been detected in observations[2,3]. Although previous studies predict an increase in heat extreme events, the magnitude of the change varies greatly among different models even for the same mean warming[4]. This uncertainty has been linked to differences in land-atmosphere feedbacks across models[2]. Here we show that a significant constraint for future projections can be based on the ability of climate models to accurately simulate the variability of daily atmospheric surface maximum temperature (TX). By applying an emergent constraint (EC) locally on a

metric describing TX variability with a large ensemble of CMIP5[5] and CMIP6[6] models we demonstrate that the best estimate increase in hot extremes could be worse than previously estimated over a large part of the land, with an increase in extremes of up to 50% larger than based on the multi-model mean. Our findings highlight the importance to correctly simulate TX variability during the historical period. Analysis of models soil moisture suggests that the EC arises because both TX variability and changes in hot extremes are related to land surface humidity processes.

Temperature extremes impact strongly on society and can have negative consequences on health[7], agriculture[8] or water resources[9]. Daily maximum temperature (TX) is often used to measure heat wave intensity. It is governed by many processes, including accumulation of solar radiation, heat transport, and sensible and latent heat flux exchange with the surface. Particularly, energy used to evaporate surface moisture can limit atmospheric warming and thus TX[10]. At any given location TX tends to be larger under drier surface conditions than wetter conditions. Another way to formulate this idea is that soil moisture (and other surface humidity variables) deficit can lead to amplified TX (and with it, potentially amplified heat waves). There is evidence that many current climate models dry too much[11] and we hypothesize that this amplifies TX variability (thus heat wave frequency[12]) whereas more accurate models may see this amplification in the upcoming decades. We postulate that this could lead to large differences between models in terms of heat wave changes under climate warming.

Many indices of TX can be used to describe hot events (as defined by Expert Team on Climate Change Detection and Indices, ETCCDI). We chose a simple derived index that can be applied easily at global scale, namely the number of days above the 98th percentile (TX98p, see methods for detailed computation). We only focus on the warmest season (June to August for North Hemisphere, December to February for South Hemisphere and all year for the 15°S-15°N tropical area). TX98p indicates for each location when a day is considered as extremely hot (relative to the daily climatology of TX at this location). By definition, it represents the 2% hottest days during the baseline period (1995-2005) at each location, and we evaluate its change in climate projections (see methods for details). We also define a metric to quantify the historical variability of TX at each location, ΔTX. This metric indicates at each grid point and for each calendar day the distance between mean TX and the 95th percentile of TX (TX95p) in degrees C. ΔTX gives an indication of the temperature difference between a hot day compared to the climatology. It is used to evaluate models against a reference dataset, ERA5 reanalysis[13]. This difference has been found to be too high in some climate models (e.g. 14). Computation of ΔTX implies that we ignore any bias in the mean TX of a model (compared to ERA5) and focus only on TX variability. Note that our results are not sensitive to using another threshold for heat wave index, e.g. the 95th percentile instead of 98th percentile (displayed in supplementary information).

Previous studies have shown that soil moisture deficits enhance surface temperature extremes[15,16] and have a strong impact on severe events such as heat waves[17]. Here we focus on daily timescale temperatures and due to limited availability of humidity model outputs at high temporal resolution (especially evaporation and integrated soil moisture are not available at daily timescales for CMIP5 outputs) we use the upper layer of soil moisture (called USM in model data, here referred to as Upper layer Soil Moisture USM for simplicity) as an indicator of land-atmosphere humidity interaction. Although USM is controlled by several factors such as infiltration, horizontal transport and evaporation (with parametrisation varying with land surface models), we assume it can be an indicator of land surface conditions during hot days. We verified that USM conditions during days above the 98th percentile exhibit a negative correlation with ΔTX over 80% of the land (Fig.S1,a), i.e. models with highest ΔTX are also drying the most. This confirms the relationship between surface humidity and TX variability during the baseline period. For some regions this relationship is not or poorly verified. This may be due to other variables influencing humidity and not included in our analysis (e.g. vegetation, deeper layer soil moisture or irrigation), specific land properties (such as permafrost for northern regions) or simply because the number of individual models for this analysis is limited. Thus even if we consider hereafter ΔTX as an indicator of model historical performances in surface humidity feedback, the physics of the relationship could be closer explored in each model.

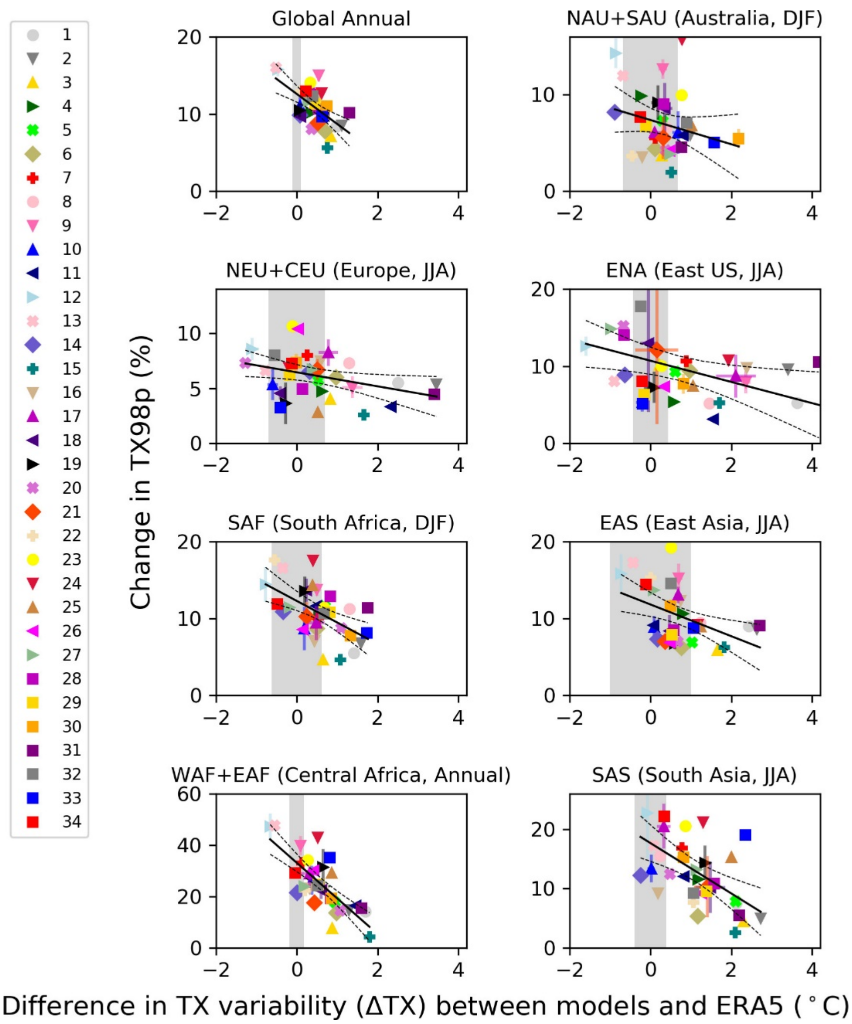

Fig.1: **Relationship between ΔTX and projected change in TX98p in selected regions**

The figure shows for each CMIP5 and CMIP6 models the change in the ensemble average frequency of hot days (TX98p, y-axis, in % of days) in the future (last decade of rcp45 and ssp245) compared to the present period (1995-2005) plotted against the a variability metric for daily maximum temperature (ΔTX) during the historical period (x-axis, in °C) averaged over different sub-regions. ΔTX measures the difference between daily TX95p and mean TX in a model compared to that observed. Solid black line is the linear regression between ΔTX and TX98p, and dashed black lines show the 95% confidence interval. Grey shading represents ΔTX uncertainties estimated from HAPPI ensemble. Acronyms refer to AR5 region definitions and numbers refer to models in Table 1.

We also verify that ΔTX is strongly correlated to TX98p change for different warming targets. Over most of land the relationship between ΔTX and TX98p change is negative (Fig.1) and significant (Fig.S2), indicating that in regions with overestimated variance for hot days the future change in TX98p is smaller on average. Thus, this simple metric is justified to constrain model projections. In the following we mask results only where ΔTX-TX98p correlation is significant. It is the case at global scale (figure 1), where the metric indicates a tendency to too large ΔTX for most models, and over most of regions except central North America, central Europe and northern polar regions.

The EC methodology requires understanding and accounting for observational and model variability and uncertainties so they it can decide how consistent they are[18]. We use the internal variability of a large multi-member historical ensembles (HAPPI) that was forced with observed sea surface temperatures to estimate ΔTX variability at each location. We then consider this information as an uncertainty range for ΔTX based on ERA5 and to evaluate when models fit within this range (with multi-member models having narrower uncertainty, see methods).

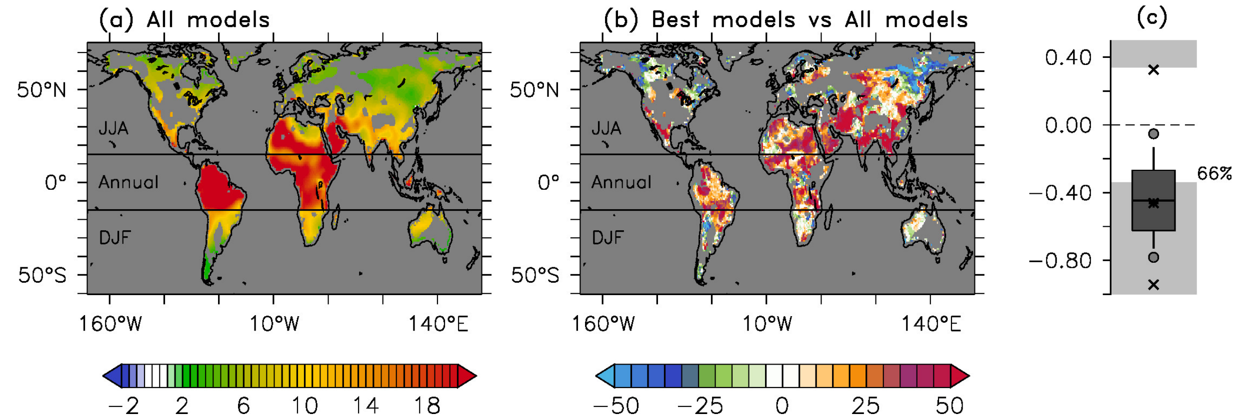

Fig2: **Implication of emergent constraint for future change in extremes**

(a) Ensemble mean (all CMIP models) difference in TX98p per degree warming compared to the baseline 1995-2005 period, expressed as a percentage of days (+X% means an extra X% of days each year will be above the 98th percentile, see methods). (b) Difference in TX98p projections between models that reproduce the observed constraint and all models, expressed as a percentage of the change in (a). (a) and (b) display results only where the correlation between TX98p and ΔTX is significant (see supplementary Fig.S2). (c) Box plot distribution of cross-models correlation coefficients between historical ΔTX and change in TX98p computed at each grid point. Dark grey box is the 25-75 interquartile, with horizontal bar inside being the median; vertical solid black line shows the 10-90 interquartile; lower and upper circle symbols are percentile 5 and 95 respectively; lower and upper cross symbols are percentile 1 and 99 respectively. Black cross in the box is the mean. Only values in light grey shading are significant at the 95% confidence level. The percentage written indicate how many grid points are above this confidence level.

Using ΔTX to constrain climate projections by selecting in each gridbox (after spatial smoothing, see methods) the models within the observed constraint, we found that changes in TX98p are larger than estimated by an unconstrained ensemble over a large part of the land (Fig.2). Africa, South and Central Asia and South America have a particularly strong signal, locally above 50% increase in the number of exceedances of the 98th percentile (although the magnitude of the difference may be partly explained by the number of selected models at each location); i.e. twice as many hot days as in unconstrained predictions. This means models representing more accurately ΔTX during baseline period (and hypothetically humidity feedbacks) tend to warm faster compared to the other models. Similar relationships are found for all climate warming targets (supplementary Fig.S11 and S12), although the area with significant correlation is reduced for 1.5°C target. This influence of our EC persists through different warming targets and is confirmed robust by several sensitivity tests (see methods).

Applying an EC based on global mean ΔTX (i.e. selecting or rejecting a single model on a global mean relationship) leads to slightly weaker, but still valid, amplification (Fig.3). Using a regional constraint to select the best models at each location seems more appropriate, as no model is considered good everywhere (supplementary Fig.S3). The constrained TX98p signal (either by local or global method) suggest that the level of increase previously estimated by the end of the century could be reached by 2060 instead, i.e. 40 years earlier. All these results are verified independent of model selection by performing sensitivity tests where one model is removed randomly from the ensemble (Fig.3). The regional constraints results remain highly consistent. The global constraint is still consistent but slightly more sensitive to model selection (due to the small size of this ensemble that fall near the uncertainty range). Thus using regional constrain method here leads to more stable and reliable results.

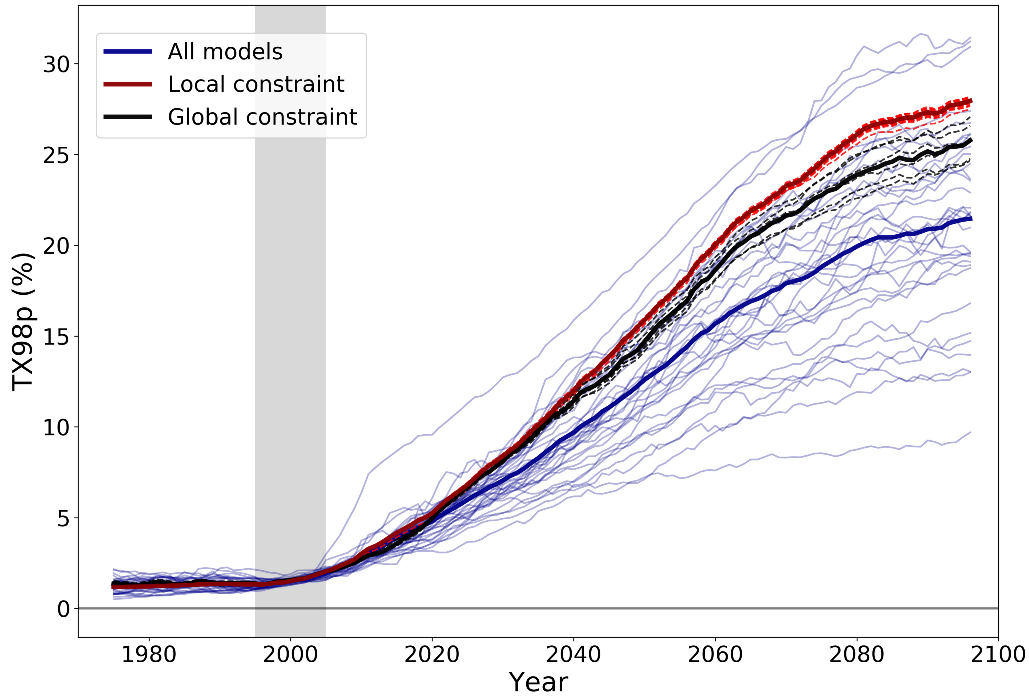

Fig.3: **Global evolution of hot extremes in unconstrained and constrained ensembles.**

Timeseries of global mean TX98p (%) for the mean (thick solid line) of all CMIP5 and CMIP6 models (blue) and constrained models with constraint applied to each significant grid point (red). Ensemble means are computed, each year, for each grid point from a 9-years running mean of TX98p, then globally averaged to obtain a global mean value. This method allows a more detailed computation of constrained ensemble, as the number of models varies from one region to another. Thin blue lines indicate individual model results. Solid back line shows the mean of a sub-ensemble (7 models) where EC is based on globally averaged ΔTX (instead of applying EC at each grid point). Gray shading highlights the baseline period to compute the TX98p threshold. Red (and black) dashed lines show a sensitivity study where one model is removed before computation of local (and global) constrained ensemble mean (test repeated for each model of each ensemble). For each model, TX98p is linearly scaled by comparing its individual change in Tas to the ensemble mean change in Tas.

An important point is to verify the physical mechanism linking change in TX98p and land drying, although due to limited data we only use monthly timescale USM outputs (i.e.

mean land drying, not specifically during hot days). The relationship between change in TX98p and mean USM is overall negative, indicating larger temperature variability for drier soils, and supporting our hypothesis (supplement material Fig.S1,b), although it is significant only over few areas and not necessarily where EC signal is the strongest (especially, it is weak over the tropical area). This may be explained by several reasons. First, USM is only one part of land moisture and does not include vegetation (which can be an important factor moderating humidity over tropical land). Secondly due the limit of USM model output data to monthly we may not capture the specific heat event well enough, making the statistical relationship more difficult to estimate. Third, a full daily analysis on evaporation, vegetation and soil moisture structure would be needed to understand how these processes changes under very specific conditions (hot days). This is obviously a strong limit to our current understanding and we can only raise a physical hypothesis. We stress here the importance of high temporal resolution surface humidity outputs to fully understand extreme event processes and humidity feedbacks.

We note that over some regions constrained models do not indicate an increase in TX98p, especially over northern part of America and Siberia. These correspond to areas with weak correlation between ΔTX and TX98p. Other processes may be more dominant in these regions, and drying of soil may be not a factor in high latitudes. Additionally, permafrost land-atmosphere exchanges and humidity processes are different there.

Overall, our results indicate that climatological bias in the difference between hot and average days in climate models lay lead to an underestimate of the frequency of unusually hot days in the future.

Acknowledgment

We acknowledge the E-OBS dataset from the EU-FP6 project UERRA (http://www.uerra.eu) and the Copernicus Climate Change Service, and the data providers in the ECA&D project (https://www.ecad.eu). This research used science gateway resources of the National Energy Research Scientific Computing Center, a DOE Office of Science User Facility supported by the Office of Science of the U.S. Department of Energy under Contract No.DE-AC02-05CH11231. This research is funded by NERC grant award NE/S004661/1 EMERGENCE project.

METHOD

Definition and computation of indices

Our analysis focusses on daily maximum temperature (TX) extremes (TX98p). We define TX98p as the number of days above the daily climatological 98th percentile. The latter is computed for each location and each calendar day by pulling together all days within +/- 15 days window of this calendar day during the 1995-2005 period and selecting the 2% highest values.

We also define a metric, ΔTX, to evaluate the variability of TX during the baseline period. It is done by first calculating the mean and 95th percentile of the temperature distribution for each calendar day at each location (by pulling 15 days around each calender day together as for 98th percentile describe above). The distance between the 95th percentile and the mean gives an indication of TX variability for each day and each location. It is computed for each model (ΔTX_{model}) and for the reference dataset (ΔTX_{ref}; the ERA5 reanalysis) and the difference between the two defines our metric: $\Delta TX = \Delta TX_{model} - \Delta TX_{ref}$. We only focus on the warm season, when hot extreme are likely to happen (June-August for North Hemisphere, December-February for South Hemisphere and all year for the 15°S-15°N tropical area). Positive values mean a model over-estimates the TX variability compared to the reference (i.e. it tends to warm up too quickly and over-estimated high values of TX), negative values indicate an underestimate. For the metric, we choose the 95th percentile to ensure reasonably good sampling of the variability across the base period (as it is used to constrain models) while for future changes we focus on the 98th percentile which correspond to more extreme values. We verified that EC results are not very sensitive to the choice of threshold by doing a sensitivity test using the 95th percentile as threshold instead 98th (supplementary Fig.S4).

Each index is computed individually for each model (and eventually each member) on their native grid. Results are then interpolated on a common 1° grid before being averaged across all models. As temperature extremes are relatively large-scale, and grids vary only between 1 and 2.5 degrees latitude/longitude across models, results are not sensitive to the order of operation.

Datasets

- CMIP models

An ensemble of 27 individual models from CMIP5[5] and 7 from CMIP6[6] is used. Some only have a single member available while some provide a multi-members ensemble. In the latter case, multi-member results are always computed individually and then averaged to provide one mean result for a single model. We consider a reference period as the historical 1995-2005 decade (being the last decade of CMIP5 historical forcing). Climate projections are investigated using the RCP4.5[19] and SSP245[20] pathways for CMIP5 and CMIP6 models respectively. Both scenarios are expected to be close, although each model leads to different mean temperature increases (Fig.S5).

Three climate projection targets are considered:

- *end-of-century*, by selecting the 2091-2100 decade for each model.

- *+1.5°C and +2°C warming above pre-industrial mean*. For these two, we follow a similar approach as in 21 and select for each member of each model the first decade when the average atmospheric surface temperature (Tas) of each year of the decade is above the corresponding threshold (Fig.S5). As we use 1995-2005 as a baseline, the actual threshold (relative to the baseline) is chosen as +0.7℃ and +1.2℃ for targets +1.5℃ and +2℃ above pre-industrial respectively, as in the HAPPI experiment design[22]. Although the exact definition of these levels can be sensitive[23], for this work the main point is that each model or member should reach a similar magnitude of warming. A few members and models do not meet the condition for the +2°C target before the end of the century. For these cases, we select instead the last projection decade 2091-2100. If the mean increase in Tas over this decade is above the threshold (+1.2° C) then we keep the model or member. Otherwise we do not include it in the analysis for this projection target. This leads us to discard 4 members.

For each climate projection target, results of each member or model are normalised by their respective mean change over the decade (relative to our baseline) in Tas (and then averaged to provide ensemble mean results). Thus, no matter the target projection all results are shown for +1C warming above the baseline. We tested the sensibility of the results by using raw results (without normalisation) for each model but both methods lead to very close results in terms of EC amplification (Fig.3 and Fig.S6), although raw results have larger uncertainties. Thus, we largely focus on normalised results in the body of the paper.

For most of the models we could get daily TX data for both historical and projection periods. Daily soil moisture data are more limited (9 CMIP5 and 5 CMIP6 models). Supplementary Table 1 provides details about outputs used for each variable.

- HAPPI ensemble and ΔTX uncertainty

To evaluate the uncertainties on ΔTX during the baseline period we use several atmospheric models from the HAPPI ensemble[22]. Each model provides daily output for the 1995-2005 decade. We select 5 models with a hundred or more members and compute ΔTX for each member (same method as for CMIP models). Then, using internal variability of each model (multi-members ensemble standard deviation, σ), we estimate ΔTX uncertainties for each location and calendar day (Fig.S7). One model has a mean bias that is much larger than other models (CanAM4), we thus exclude it. For other models, the ΔTX internal variability is consistent, so we use the mean of four remaining model variabilities (i.e. averaging the four internal STD) as a measure of ΔTX uncertainties (σ_{HAPPI}).

The sensitivity of this choice is also tested by using individual model STD instead of ensemble mean (Fig.S8). It shows that results stay consistent for each case. We note that the uncertainty so described is that of atmospheric variability only. However, both the HAPPI ensemble and the ERA5 reanalysis are driven by the same SSTs hence this choice is conservative to characterize observational uncertainty.

Internal variability in the climate models used is reduced by ensemble averaging. To take into account the specific number of members for each individual model, the uncertainty between OBS and models is expressed as: $(\sigma^2_{HAPPI} + (\sigma^2_{HAPPI} / N))^{1/2}$ with N the number of members of a model. When the absolute value of ΔTX fits within that range then a model (eventually the multi-members ensemble mean) is considered as consistent with OBS.

- ERA5

The ERA5 reanalysis[13] is available for the full satellite observation period (1979-present). It provides hourly timescales data at 0.25° resolution on a reduced Gaussian grid, from which we computed daily TX for the 1995-2005 period.

We evaluated the variability of TX in ERA5 against two dense regional observational datasets (Fig.S9): A network of 756 homogenised station measurements for China, provided by the Chinese Meteorological Administration[24]; And gridded 0.25° E-OBS v19.0 dataset for Europe[25]. Chinese observations are first gridded on the same regular grid as ERA5 by linear interpolation.

Although the TX variability tends to be weaker in ERA5 than in observations, differences are within the range of uncertainties estimated from the HAPPI ensemble variability (Fig.S7) for both regions, hence we consider ERA5 sufficient.

Emergent constraint (EC) method

To decrease model projection uncertainties on TX98p, we use an EC method with ΔTX as a predictor (i.e. selecting models that are able to reproduce the width of the daily maximum temperature distribution TX, indicated by the distance between the 95th percentile and the median) and select those for prediction. To do this, CMIP models are evaluated against ERA5 during the 1995-2005 period, and agree with it within atmospheric internal variability. We use variability from the HAPPI ensemble to characterize this uncertainty for better sampling. Models (ensemble mean in case of multi-members model) within the range of 2 times STD (i.e. the 95% confidence interval) are considered as reasonably realistic and selected for use in the constrained climate projections. Comparing constrained against unconstrained ensemble projections provides an estimate of the potential current bias in climate forecasts.

Constraints can arise from global or regional processes[18]. Here we use a regional constraint to take advantage of model information everywhere. We first apply a spatial smoothing of 5 degrees on ΔTX over land (to improve sampling and avoid spatial discontinuity) then select the models that comply with the constraint within uncertainty at each grid point. Over most of the regions, the number of selected models is between 5 and 10, except in central Africa where it is below 5. This is mainly due to very narrow observational variability over this region (Fig.S3 and S7). Most of models contribute to the projection over some part of land. Applying EC at a global scale instead (Fig.3 and S10) leads to similar patterns with slightly weaker amplification.

We also tested the sensitivity of EC results with different choices of uncertainty around the observational distribution with and different spatial smoothing (Fig.S8). Using narrower (wider) range of variability leads to slightly different results with less (more) models selected, corresponding to a noisier but more intense (smoother but less intense) signal. However, global patterns are still consistent with main results. Weaker spatial smoothing (3 degrees) leads to slightly nosier results while using too large smoothing (11 degrees) leads to large masked area (because we use only land grid points or alternatively to large variation in actual applied smoothing). Thus 5 degrees smoothing is a good compromise.

Following recommendations from Hall et al., 2019, we first confirm the strong statistical relationship between ΔTX and TX98p (Fig.1 and supplement S2). We then use a resampling method (by removing randomly a model from the ensemble) to test the robustness of the constraint (Fig.3). Finally, the physical mechanism hypothesis linking soil moisture, ΔTX and TX98p is evaluated (Fig.S1), although this evaluation is somewhat limited due to limited soil moisture availability.

Data availability

The authors declare that all data that support the findings in the main article are available. All model data are publicly accessible via the Earth System Grid Federation node (https://esgf-node.ipsl.upmc.fr/). ERA5 data can be downloaded from ECMWF website (https://www.ecmwf.int/en/forecasts/datasets/reanalysis-datasets/era5). Scripts used to generate the main results will be made available on the University of Edinburgh datashare. All other data and code that support the figures in the Supplementary Information are available from the corresponding author on request.

References

1: Herring, S. C., Hoerling, M. P., Kossin, J. P., Peterson, T. C., & Stott, P. A., Explaining extreme events of 2014 from a climate perspective. Bulletin of the American Meteorological Society, **96**(12), S1-S172, 2015

2: Seneviratne, S. I., et al., Changes in climate extremes and their impacts on the natural physical environment.. Managing the risks of extreme events and disasters to advance climate change adaptation: Special report of the Intergovernmental Panel on Climate Change, 109-230, 2012

3: Bindoff, N.L., Stott, P.A., AchutaRao, K.M., Allen, M.R., Gillett, N., Gutzler, D., Hansingo, K., Hegerl, G., Hu, Y., Jain, S. and Mokhov, I.I., CH10: Detection and attribution of climate change: from global to regional, 2013

4: Hoegh-Guldberg and Coauthors, CH3: Impacts of 1.5°C global warming on natural and human systems, 2018

5: Taylor, K.E., R.J. Stouffer, G.A. Meehl, An Overview of CMIP5 and the experiment design. Bull. Amer. Meteor. Soc., **93**, 485-498, 2012

6: Eyring, V., Bony, S., Meehl, G. A., Senior, C. A., Stevens, B., Stouffer, R. J., & Taylor, K. E., Overview of the Coupled Model Intercomparison Project Phase 6 (CMIP6) experimental design and organization. Geoscientific Model Development (Online), **9**, LLNL-JRNL-736881, 2016

7: Guo, Y., A., Gasparrini, B. G. Armstrong and Coauthors, Heat wave and mortality: a multicountry, multicommunity study. Environmental health perspectives, **125**(8), 087006, 2017

8: Vogel, E., Donat, M. G., Alexander, L. V., Meinshausen, M., Ray, D. K., Karoly, D., Meinshausen, N. & Frieler, K., The effects of climate extremes on global agricultural yields. ERL, **14**(5), 054010, 2019

9: Zuo, J., Pullen, S., Palmer, J., et al., Impacts of heat waves and corresponding measures: a review. Journal of Cleaner Production, 1-12, 2015

10: Whan, K., Zscheischler, J., Orth, R., Shongwe, M., Rahimi, M., Asare, E. O., & Seneviratne, S. I., Impact of soil moisture on extreme maximum temperatures in Europe. Weather and Climate Extremes, **9**, 57-67, 2015

11: Milly, P. C. D. and Dunne, K. A., Potential evapotranspiration and continental drying. Nature Clim. Ch., **6**, 946-949, 2016

12: Schär, C., P. L. Vidale, D. Lüthi, C. Frei, C. Häberli, M. A. Liniger and C. Appenzeller, The role of increasing temperature variability in European summer heatwaves. Nature, **427**, 332-336, 2004

13: Hersbach and Coauthors, Operational global reanalysis: progress, future directions and synergies with NWP. European Centre for Medium Range Weather Forecasts, 2018

14: Hanlon H., Hegerl, G.C., Tett, S.F.B., Smith, D. , Can a decadal forecasting system predict temperature extreme indices?. J. Climate, **26**, 3728-3744, 2013

15: Seneviratne, S.I., Corti, T., Davin, E.L., Hirschi, M., Jaeger, E.B., Lehner, I., Teuling, A.J., Investigating soil moisture–climate interactions in a changing climate: a review. Earth-Sci. Rev., **99**(3), 125-161, 2010

16: Seneviratne, S. I., Wilhelm, M., Stanelle, T., van den Hurk, B., Hagemann, S., Berg, A., ... & Claussen, M., Impact of soil moisture-climate feedbacks on CMIP5 projections: First results from the GLACE-CMIP5 experiment. Geophysical Research Letters, **40**(19), 5212-5217, 2013

17: Miralles, D. G., Gentine, P., Seneviratne, S. I., & Teuling, A. J., Land–atmospheric feedbacks during droughts and heatwaves: state of the science and current challenges. Annals of the New York Academy of Sciences, **1436**(1), 19, 2019

18: Hall, A., Cox, P., Huntingford, C., & Klein, S. , Progressing emergent constraints on future climate change. Nature Climate Change, 2019

19: van Vuuren DP, JA Edmonds, M Kainuma, K Riahi, AM Thomson, K Hibbard, GC Hurtt, T Kram, V Krey, J-F Lamarque, T Masui, M Meinshausen, N Nakicenovic, SJ Smith, and S Rose, The representative concentration pathways: an overview Climatic Change. **109**(1-2), 5-31, 2011

20: Gidden, M., Riahi, K., Smith, S., Fujimori, S., Luderer, G., Kriegler, and Coauthors, Global emissions pathways under different socioeconomic scenarios for use in CMIP6: a dataset of harmonized emissions trajectories through the end of the century. Geoscientific Model Development Discussions, **12**(4), 1443-1475, 2019

21: King, A. D., Knutti, R., Uhe, P., Mitchell, D. M., Lewis, S. C., Arblaster, J. M., & Freychet, N., On the linearity of local and regional temperature changes from 1.5 C to 2 C of global warming. Journal of Climate, **31**(18), 7495-7514, 2018

22: Mitchell, Daniel, Krishna AchutaRao, I. Bethke, U. Beyerle, Andy Ciavarella, P. M. Forster, Jan Fuglestvedt et al., Half a degree additional warming, prognosis and projected impacts (HAPPI): background and experimental design. Geoscientific Model Development, **10**, 571-583, 2017

23: Schurer, A. P., Cowtan, K., Hawkins, E., Mann, M. E., Scott, V., & Tett, S. F. B. , Interpretations of the Paris climate target. Nature Geoscience, **11**(4), 220, 2018

24: Li Z. and Z.-W. Yan, Homogenized daily mean/maximum/minimum temperature series for China from 1960-2008. Atmospheric and Oceanic Science Letters, **2**(4), 237-243, 2009

25: Cornes, R., G. van der Schrier, E.J.M. van den Besselaar, and P.D. Jones, An Ensemble Version of the E-OBS Temperature and Precipitation Datasets. J. Geophys. Res. Atmos., **123**, 2018

369